Appl. Phys. B 79, 725–729 (2004)
DOI: 10.1007/s00340-004-1607-2

Applied Physics B
Lasers and Optics

G. MOURET[1,✉]
S. MATTON[1]
R. BOCQUET[1]
F. HINDLE[1]
E. PEYTAVIT[2]
J.F. LAMPIN[2]
D. LIPPENS[2]

Far-infrared cw difference-frequency generation using vertically integrated and planar low temperature grown GaAs photomixers: application to H_2S rotational spectrum up to 3 THz

[1] Laboratoire de Physico Chimie de l'Atmosphère, UMR CNRS 8101, Université du Littoral Côte d'Opale, 145 Avenue Maurice Schumann, 59140 Dunkerque, France
[2] Institut d'Electronique et de Microélectronique de Nanotechnologie, UMR CNRS 8520, Université des Sciences et Technologies de Lille, Avenue Poincaré, BP 69, 59652 Villeneuve d'Ascq Cedex, France

Received: 6 February 2004/Revised version: 30 June 2004
Published online: 8 September 2004 •

ABSTRACT The generation of continuous coherent THz radiation by mixing two cw Ti:Sa laser beams with a well-controlled frequency separation for a new scheme of vertically integrated low temperature grown GaAs (LTG-GaAs) spiral photomixer is reported. For this new photomixer device used in THz emission, the LTG-GaAs active layer is sandwiched between the two parallel metal plates of a high-speed photodetector loaded by a broadband spiral antenna. We have exploited the advantage of a higher delivered power in the low part of the spectrum (< 2000 GHz), while a low RC time constant planar interdigitated detector was used at the upper frequency. The performances of the spectroscopic setup in terms of spectral resolution (5 MHz), tunability and frequency capability are assessed by measurements of the pure rotational spectra of hydrogen sulfide (H_2S) up to 3000 GHz.

PACS 73.40.Sx; 33.20.Bx; 39.30.+w

1 Introduction

Submillimetre wavelengths and the far-infrared region extend from 1 mm to 30 μm, corresponding to frequencies from 100 GHz to 10 THz. This frequency range still remains relatively unexploited and has often been qualified as the 'spectral gap' due to the considerable difficulties to produce tunable THz radiation, hampering various applications.

New opportunities appear, connected to the considerable progress realised in the elaboration of non-linear crystals and/or semiconductors. Particularly, ultra-fast devices using low temperature grown GaAs (LTG-GaAs) have strong potential. Firstly, the joint use of LTG-GaAs and ultra-short optical pulses can produce and detect broadband THz pulse radiation. Time domain spectroscopy (TDS) experiments have been extensively employed and provide a useful method to study absorption and dispersion of various samples in the THz frequency range [1]. Properties of dielectrics, semiconductors, gases, liquids and flames have been studied by this latter method, which presents a very wide spectral coverage, however with a poor spectral resolution. When superior spectral resolution is required a different approach must be adopted, for example the production of continuous THz by mixing two visible laser beams in a LTG-GaAs photodetector known as photomixing.

Free-space THz radiation obtained by photomixing using a LTG-GaAs mixer was first demonstrated by Brown et al. in 1995 to generate output radiation up to 3.8 THz [2, 3]. This new tunable THz source has been subsequently used to study SO_2 self-broadening between 100 GHz and 1000 GHz. This experiment was limited in the upper electromagnetic spectrum by a poor signal to noise ratio above 1000 GHz due to the mixer element and the 584-nm pump wavelength, while the efficiency is maximum over the range 780–852 nm [4]. A compact photomixing THz spectrometer using diode lasers as pumping source has extended spectroscopic measurements up to 1.5 THz [5]. Diode lasers have numerous advantages, such as small size, low power consumption and long lifetime but present a limited fine-tuning range without mode hop. Diode lasers have also been used to demonstrate that the photomixing could make a good candidate in a local oscillator heterodyne receiver. Operation at 630 GHz by using a niobium superconducting tunnel junction has been reported [6]. By using a more sophisticated antenna design, like a dual antenna, higher output power has been obtained in a smaller tuning bandwidth [7].

In this paper, we present for the first time to our knowledge the performances of a new scheme of photomixer, by comparing them with a standard planar device. We show that by exploiting two different LTG-GaAs photomixers and the well-known tunability of a Ti:Sa laser, a versatile bench-top THz spectrometer with a very wide tuning range can be obtained. The characteristics of the THz spectroscopic setup in terms of spectral resolution, tunability and frequency capability are assessed by measurements of the pure rotational spectra of hydrogen sulfide (H_2S) up to 3000 GHz. Finally, the air broadening of a discrete rotational absorption line is reported.

2 Photomixing experiment

2.1 *Principle of the photomixing*

When two linearly polarised optical signals are mixed in a photodetector, the optical power modulation enve-

✉ Fax: +33-3-2865-8244, E-mail: mouret@univ-littoral.fr

lope induces a time-dependent photocurrent at the difference between optical frequencies ($\Delta\nu$) to produce a submillimetre wave power, which can be expressed as

$$P_{\Delta\nu} = Z \times [i_{\Delta\nu}]^2_{\mathrm{rms}} \,, \tag{1}$$

with

$$[i_{\Delta\nu}]_{\mathrm{rms}} = R_{\mathrm{dc}}\varrho\sqrt{2P_1P_2}\cos\left(\phi_{\mathrm{p}}\right) \,. \tag{2}$$

Here $[i_{\Delta\nu}]_{\mathrm{rms}}$ is the root-mean-square difference frequency photocurrent induced in the photomixer, whereas the direct current (dc) is ignored in (2), since it does not contribute to the THz emission. P_1 and P_2 are powers of the individual lasers and ϕ_{p} is the angle between their polarisations. R_{dc} is the dc responsivity of the detector and ϱ is a dimensionless photodetector frequency response which tends to 1 as $\Delta\nu$ tends to 0. This latter coefficient depends on the intrinsic lifetime of photocarriers as well as the antenna characteristics used to radiate THz radiation. A Si hyperhemispherical lens is usually used as collection optics, and ϱ should also describe the non-uniform coupling efficiency versus frequency of such devices [8]. Z indicates the impedance of the radiating antenna, which is considered independent of the difference frequency between the two lasers. Quadratic relations between the output THz power and (P_1P_2) and the bias voltage across the photomixer will be used to obtain a sufficient signal to noise ratio for future experiments.

2.2 *Photomixer details*

In this present demonstration, we have derived benefit from two different photomixers. The conventional planar structure photomixer consists of a 8×8 μm interdigital electrode array with 0.2-μm fingers spaced by 1.8-μm gaps coupled to a log-spiral antenna proposed by McIntosh et al. [3]. We have implemented a second photomixer in order to avoid some unwanted and tedious two-dimensional effects. In this structure, the 1.8-μm LTG-GaAs active layer is sandwiched between the two parallel metal plates of the photodetector. The top part is an Au semi-transparent electrode and the lower component is a thick metal overlay. Each 5×5 μm^2 electrode is attached to an arm of a similar broadband spiral antenna as that used in the planar approach. Process fabrication and a detailed description are reported in [9, 10]. In this vertical configuration, the photocurrent is produced only in the active layer and contributions from the substrate are avoided, which could reduce the ultimate bandwidth. In addition, a vertical photomixer seems to be much more reliable by avoiding the electrical peak strength due to uniform field operating conditions. The photocurrent is distributed in a greater volume, and could facilitate thermal dissipation.

The active-layer material used for the present experiments was grown by gas-source molecular beam epitaxy. Starting from a semi-insulating (100) GaAs substrate, a buffer layer was firstly grown at the nominal temperature of 600 °C followed by the growth of a 1-μm-thick LTG-GaAs layer. The growth temperature was around 200 °C and subsequent annealing was carried out at 600 °C for 1 min. The sample was characterised by time-resolved photoreflectivity using a mode-locked femtosecond Ti:Sa laser and a subpicosecond time constant was observed.

2.3 *Experimental setup*

A schematic overview of the THz setup is shown in Fig. 1. Two commercial cw Ti:sapphire lasers (899-29 Autoscan, Coherent, Inc.), tunable from 700 to 810 nm and 790 to 910 nm, were both pumped by a 23-W argon laser. Each of them is locked onto one Fabry–Pérot étalon cavity using a commercial edge-servo control. For the present demonstration, the wavelength of the two lasers was around 800 nm. A half-wave plate and a polariser were used to carefully adjust the laser pump power. The two laser beams were spatially overlapped using a beam splitter and fed into a single-mode polarisation-maintaining optical fibre. This improves the mode matching to obtain an optimum mixing efficiency. An objective lens (×20, 0.4 NA) is used to focus the laser beams onto the THz photomixer. It is worthwhile noting that the direction of the linear polarisation of both pump laser beams must be perpendicular to the fingers of the mixer to optimise the photocurrent, and inherently the power-conversion efficiency. Small dimensions of the interdigitated array can play the role of a grid polariser, which may explain this preferential polarisation direction on the photomixer. The THz emission was precollimated by a silicon lens attached to the back side of the chip and focused with a parabolic mirror onto a Si composite bolometer that operates at 4.2 K. The output signal from the detector was monitored using a lock-in amplifier.

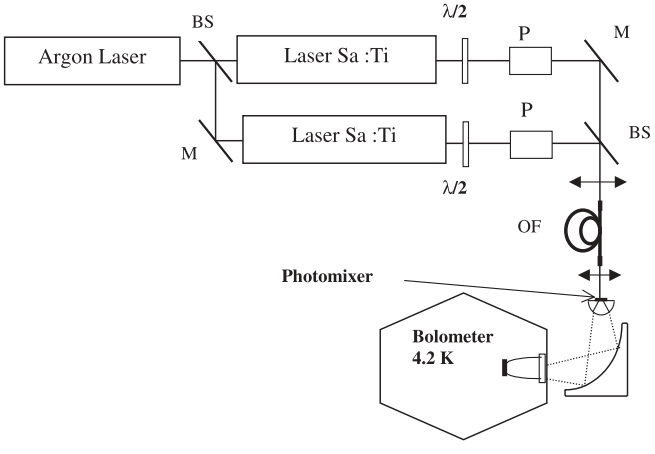

FIGURE 1 Experimental setup of the photomixing experiment: BS, beam splitter; M, mirror; λ/2, half-wave plate; P, polariser; OF, optical fibre

3 Results

Figure 2 shows a first comparison of the radiated power for planar and vertical configurations. Experimental conditions are not identical, so the comparison is not immediate. Nevertheless, THz radiation is produced over more than one decade of frequency for the two structures, with a strong decrease in power from 800 GHz.

First, the responsivity of the vertical photomixer is superior to that of the planar geometry. A responsivity of

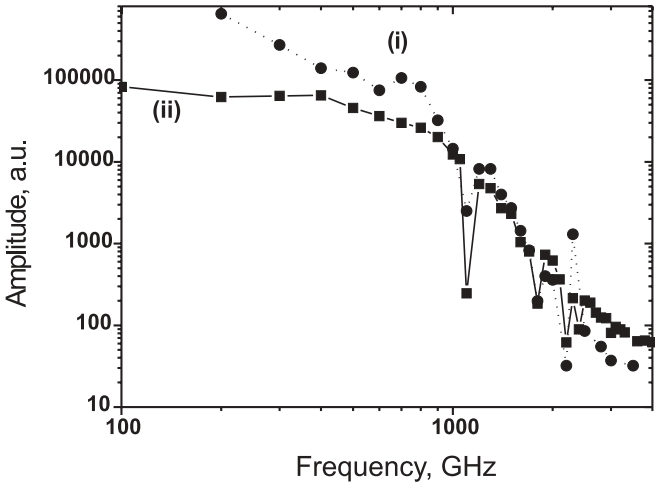

FIGURE 2 THz power plotted versus the difference frequency between the two lasers. (i) Vertical configuration with 10-V bias and 80-mW optical pump power. (ii) Standard planar photomixer with 5-V bias and 35-mW optical pump power

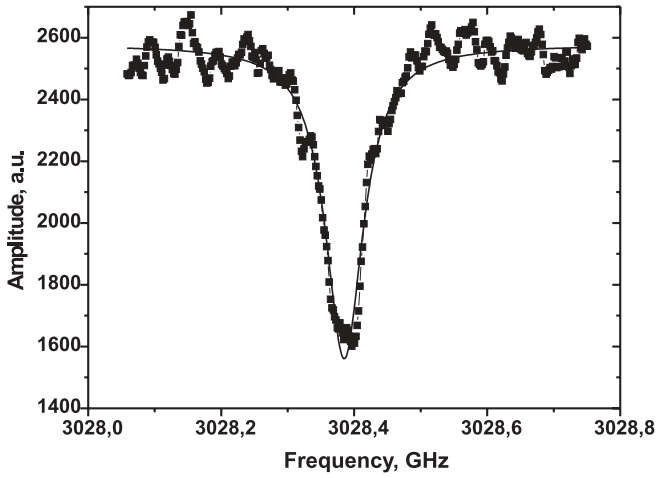

FIGURE 3 The $5_{0,5} \rightarrow 4_{4,1}$ hydrogen sulfide absorption line centred at 3028.388 GHz recorded at 0.4 mbar

0.035 A/W was obtained against 0.005 A/W for the planar structure with a total pump power of 20 mW and a bias voltage of 4 V. In the same conditions, more photocurrent is produced by the vertical configuration, which therefore has a better conversion efficiency.

In this present demonstration, and in fact at frequencies up to 1.8 THz, more output THz power is detected by using the new structure. For example, at 1300 GHz the new structure radiates twice the power of the conventional configuration. However, at ultimate frequencies, higher intrinsic capacity results in the planar structure radiating more THz power compared with the vertical structure. The maximum THz detected power in the lower part of the spectrum (around 200 GHz) has been estimated to be around 1 μW using a Si cryogenic bolometer assuming a responsivity of 12 kV/W obtained from a calibration at 275 GHz using a black-body source and a band-pass filter. Estimation of measurement precision is problematic due to the lack of calibrated sources at THz frequencies. THz detected power decreases with increasing frequency, with a slope of 12–15 dB/octave. A few tens of pW are available beyond 3 THz, which are sufficient to perform absorption spectroscopy by exploiting the excellent noise characteristics of cryogenic detectors (NEP $\approx$ 2.8 pW $Hz^{-1/2}$). The behaviour of the planar device is in accordance with the model in Sect. 2 with regard to the quadratic dependence of the detected THz power with both the pump power and the bias voltage. The new vertical structure is in good agreement with the model at low bias voltage, whereas measurements performed at high bias voltage deviate from it. The higher direct photocurrent does not correspond with the higher detected THz power and the dc responsivity is no longer a relevant characteristic to evaluate the photomixer. A non-steady-state velocity-overshoot effect is expected and explained in [10].

3.1 *Spectroscopic application: higher-frequency limit*

To investigate the potential capability of the photomixing spectrometer in the higher part of the spectrum, we have recorded a hydrogen sulfide absorption line above 3000 GHz (Fig. 3) by using a 1-m absorption cell inserted between the photomixer and the bolometer. The planar structure was used in this first experiment due to its better performance at this frequency. This figure points out the ultimate capabilities for a photomixing experiment, in good agreement with remarks stated in [4].

3.2 *Spectroscopic application: spectral purity of the source*

With this technique, the spectral purity of the THz radiation is the convolution of line widths of the two optical pump lasers and so is a function of the laser frequency stabilisation schemes. To estimate the practical THz source line width, we have resolved two hydrogen sulfide lines, which have not been resolved previously and are not present in the database [11]. The transitions $6_{0,6} \rightarrow 5_{1,5}$ and $6_{1,6} \rightarrow 5_{0,5}$ are clearly resolved in Fig. 4. The source line width is estimated to be around 5 MHz, confirmed by direct measurements of the beat note by using a photodetector and a microwave spectrum analyser, when the two Ti:Sa laser frequencies are tuned to obtain a difference in the microwave region. The frequency sepa-

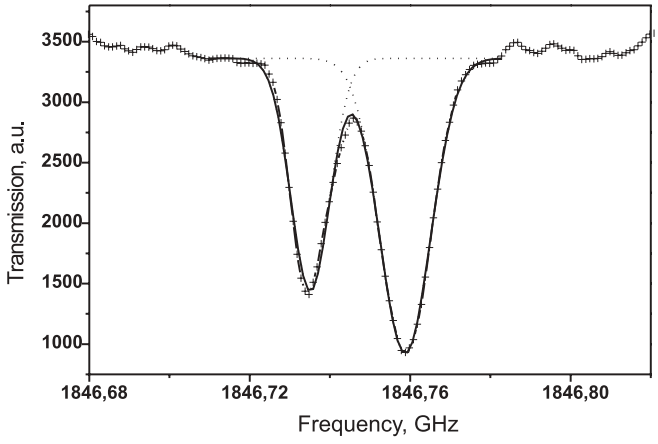

FIGURE 4 High-resolution scan. The $6_{0,6} \rightarrow 5_{1,5}$ and $6_{1,6} \rightarrow 5_{0,5}$ transition lines are clearly resolved and are separated by 23.7 MHz. The pressure was 0.03 mbar

ration between these two transitions is estimated to 23.7 MHz by use of a Lorentzian fit. An improvement of the stability could be achieved usually at the expense of the tunability.

3.3 *Spectroscopic application: scanning performance and absolute frequency knowledge*

Due to the well-known tunability of Ti:Sa lasers, large frequency scans can be performed, which provide the possibility to calibrate the absorption spectrum by using one or several reference absorption lines. A 40-GHz absorption spectrum around 1500 GHz is presented in Fig. 5. Standard lines can be found in databases, which have been measured with an extreme accuracy. The combination of an absolute reference and a Fabry–Pérot etalon gives the possibility to generate calibration markers in the THz spectrum, in order to check the linearity of the scan and to perform an interpolation for frequency measurement. The deviations of measured spectral line frequencies from database values were estimated to be around 4 MHz, by examining the reproducibility of successive scans. This poor value, which is still inconsistent with high-resolution THz spectroscopy, is due to the low-frequency drift (30 MHz/h) of the fixed laser. We plan to improve this present arrangement by locking the fixed laser onto an absolute frequency reference (such as an atomic transition). At the present time, it is locked onto a Fabry–Pérot interferometer which naturally has a temperature dependence. The THz frequency measurement has been solved by Matsuura et al., who have obtained an absolute calibration of 10^{-7} [12]. This method has been used to measure the rotational spectrum of water between 841 and 1575 GHz [13].

3.4 *Spectroscopic application: air-broadening parameter*

However, the scan linearity is sufficient to measure some parameters of a discrete absorption line. We have used the present THz photomixing spectrometer to measure the H_2S air broadening of the $4_{1,4} - 3_{0,3}$ transition centred at 1281.711 GHz. Hydrogen sulfide plays an important role in the global environment; it is converted rapidly to SO_2 that is ultimately oxidised to sulfuric acid, the major contributor to acid precipitation. This compound exhibits a very intense rotational spectrum in the submillimetre wavelengths, which would be potentially interesting to survey this pollutant, and thus requires a good knowledge of collisional properties which are usually much less well known than transition frequencies [14].

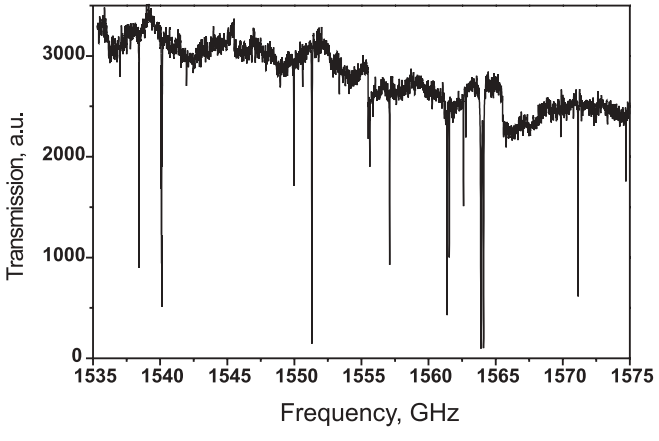

FIGURE 5 A 40-GHz hydrogen sulfide absorption spectrum recorded at 0.4 mbar

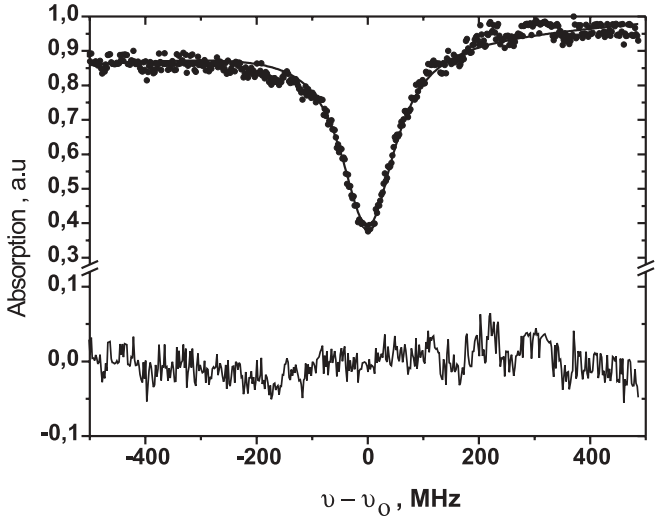

FIGURE 6 Absorption line shape recorded at a total pressure of 17.5 mbar

An initial pressure of 0.1 mbar was introduced in the absorption cell and we recorded a series of scans at various pressures from 4 mbar to 30 mbar by adding air. Pressures were measured with two capacitance manometers, depending on the pressure range. Figure 6 shows an example of a recorded line shape at a total pressure of 17.5 mbar. The line shape has been fitted by a least-square method to a Lorentzian profile to extract the collisional width. The equation used for the fit is

$$\frac{I(\nu)}{I_0} = A_3 + A_4\Delta\nu + \exp\left[\frac{A_1 A_2}{\pi\left(\Delta\nu^2 + A_2^2\right)}\right]. \qquad (3)$$

It takes into account a linear baseline $(A_3 + A_4\Delta\nu)$ and a nonlinear absorption line $(\exp\left[A_1A_2/(\pi(\Delta\nu^2 + A_2^2))\right])$. The coefficient A_2 corresponds to the half width at half maximum (HWHM) for the Lorentzian profile. The signal to noise ratio of the transition is sufficient to give a good agreement between the fit and the experimental data. The difference, as shown in the lower part of the figure, is always below 5% and is dominated by residual baseline component. The air-broadening coefficient was estimated to be 2.64 MHz/mbar (HWHM) at room temperature.

4 Conclusion

In comparison with a standard planar photomixer, the characteristics of a new vertically integrated photomixer were demonstrated versus the standard device. The power capabilities of this new device are much more attractive up to 1.8 THz. Through spectroscopic measurements, the performances and limits of the photomixing experiment have been presented. Particularly, we have pointed out the possibility of using the photomixing technique to perform spectroscopic measurements up to 3000 GHz. The $5_{0,5} \rightarrow 4_{4,1}$ hydrogen sulfide absorption line centred at 3028.388 GHz has been clearly

recorded. In addition, the H_2S air broadening of the $4_{1,4} - 3_{0,3}$ transition was reported. The major drawback is the poor THz output power, which still requires cryogenic detectors mainly at ultimate frequency. And, the prospects for the vertical scheme to exploit transfer techniques appear promising by improvement of thermal management and subsequently the power capabilities.

ACKNOWLEDGEMENTS This work was supported by the French Research Ministry via the Action Concertée Incitative (ACI) GOTIC.

REFERENCES

1 D. Mittleman: *Sensing with THz Radiation* (Springer, Berlin, Heidelberg 2003)
2 E.R. Brown, K.A. McIntosh, K.B. Nichols, C.L. Dennis: Appl. Phys. Lett. **66**, 285 (1995)
3 K.A. McIntosh, E.R. Brown, K.B. Nichols, O.B. McMahon, W.F. Dinatale, T.M. Lyszczarz: Appl. Phys. Lett. **67**, 3844 (1995)
4 A.S. Pine, R.D. Suenram, E.R. Brown, K.A. McIntosh: J. Mol. Spectrosc. **175**, 37 (1998)
5 S. Matsuura, M. Tani, H. Abe, K. Sakai, H. Ozeki, S. Saito: J. Mol. Spectrosc. **187**, 97 (1998)
6 S. Verghese, E.K. Duerr, K.A. McIntosh, S.M. Duffy, S.D. Colowa, C.E. Tong, R. Kimberg, R. Blundell: IEEE Microwave Guid. Wave Lett. **9**, 245 (1999)
7 S.M. Duffy, S. Verghese, K.A. McIntosh: IEEE Trans. Microwave Theory Tech. **49**, 1032 (2001)
8 J. Van Rudd, D. Mittleman: J. Opt. Soc. Am. B **19**, 319 (2002)
9 E. Peytavit, G. Mouret, J.F. Lampin, S. Arscott, P. Masselin, L. Desplanque, O. Vanbésien, R. Bocquet, F. Mollot, D. Lippens: IEE Spec. Issue Fast Optoelectron. **149**, 82 (2002)
10 E. Peytavit, S. Arscott, D. Lippens, G. Mouret, S. Matton, P. Masselin, R. Bocquet, J.F. Lampin, L. Desplanque, F. Mollot: Appl. Phys. Lett. **81**, 1174 (2002)
11 H.M. Pickett, R.L. Poynter, E.A. Cohen: *Submillimeter, Millimeter and Microwave Spectral Line Catalog*, accessed via World Wide Web (http://spec.jpl.nasa.gov) from the Jet Propulsion Laboratory, Pasadena, CA
12 S. Matsuura, P. Chen, G.A. Blake, J.C. Pearson, H.M. Pickett: IEEE Trans. Microwave Theory **48**, 1301 (2000)
13 P. Chen, J.C. Pearson, H.M. Pickett, S. Matsuura, G.A. Blake: Astrophys. J. **128**, 371 (2000)
14 G. Mouret, W. Chen, D. Boucher, R. Bocquet, P. Mounaix, D. Lippens: Opt. Lett. **24**, 351 (1999)